Electronic Supplementary Information (ESI) for

Two coordination polymers as multi-responsive luminescent sensors for detection of UO_2^{2+}, Cr(VI), and NFT antibiotic

Yun-Shan Xue,[a] Dan-Ling Sun,[a] Jun-Qing Lv,[a] Shi-Juan Li,[a] Xuan-Rong Chen,[a] Wei-Wei Cheng,[b] Hong-Xiu Wu, [*a] Jun Wang[*a]

[a]*School of Chemistry & Environmental Engineering, Yancheng Teachers University, Yancheng, 224007, China.*
[b]*School of Chemistry and Bioengineering, Nanjing Normal University Taizhou College, Taizhou 225300, China.*

E-mail: wjyctu@hotmail.com; sunnywuxh@163.com.

Table of Contents

1. Experimental section

2. Tables

Table S1. Crystallographic Data collection and Refinement result for compounds **1-2**.

Table S2. Selected bond lengths (Å) and angles (deg) for compounds **1-2**.

Table S3. Standard deviation and detection limit calculation for UO_2^{2+}, Cr(VI) and NFT in **1**.

Table S4. Standard deviation and detection limit calculation for UO_2^{2+}, Cr(VI) and NFT in **2**.

Table S5. Comparison of various CPs sensors for the detection of Cr(VI) ions.

Table S6. Comparison of various CPs sensors for the detection of UO_2^{2+} ion.

Table S7. Comparison of various CPs sensors for the detection of NFT.

3. Figures

Fig. S1 The simplified network of compound **1**.

Fig. S2 4,5-connected 3D network of compound **2**.

Fig. S3 PXRD pattern of compound **1**: (a) simulated, (b) experimental.

Fig. S4 PXRD pattern of compound **2**: (a) simulated, (b) experimental.

Fig. S5 TGA curves for compounds **1-2**.

Fig. S6 pH-dependent emission spectra of compound 1 (a) and compound 2 (c) in the aqueous solution with pH ranging from 1 to 13; Histogram showed fluorescence emission of compound 1 (b) and compound 2 (d) at different pH values.

Fig. S7 Luminescence intensities of compound 1 (a, c) and 2 (b, d) with different mixed ions solution added $Cr_2O_7^{2-}$ / CrO_4^{2-} anions (m1: PO_4^{3-} / HPO_4^{2-}; m2: CO_3^{2-} / HCO^{3-}; m3: SO_4^{2-} / $C_2O_4^{2-}$; m4: SCN^- / NO_3^-; 1 mM).

Fig. S8 Luminescence intensities of compound 1 (a) and 2 (b) with different mixed ions solution added UO_2^{2+} ion (m1: $K^+/Ca^{2+}/Mg^{2+}$; m2: Zn^{2+}/Cd^{2+}; m3: Co^{2+}/Ni^{2+}; m4: Ag^+/Na^+; m5: Cr^{3+}/Cu^{2+}; 1 mM)

Fig. S9 PXRD pattern of compound 1 after immersing into water with different analytes.

Fig. S10 PXRD pattern of compound 2 after immersing into water with different analytes.

Fig. S11 UV-vis spectra of different anions in aqueous solutions, and the excitation and emission spectra of compounds 1-2.

Fig. S12 UV-vis spectra of different metal ions in aqueous solutions, and the excitation and emission spectra of compounds 1-2.

Fig. S13 The HOMO and LUMO energy levels for different antibiotics and ligands.

Fig. S14 Fluorescence decay for compound 1 (λ_{ex} = 300 nm).

Fig. S15 Fluorescence decay for compound 1 in the presence of $Cr_2O_7^{2-}$.

Fig. S16 Fluorescence decay for compound 1 in the presence of CrO_4^{2-} (λ_{ex} = 300 nm).

Fig. S17 Fluorescence decay for compound 1 in the presence of UO_2^{2+} (λ_{ex} = 300 nm).

Fig. S18 Fluorescence decay for compound 1 in the presence of NFT (λ_{ex} = 300 nm).

Fig. S19 Fluorescence decay for compound 2 (λ_{ex} = 300 nm).

Fig. S20 Fluorescence decay for compound 2 in the presence of $Cr_2O_7^{2-}$ (λ_{ex} = 300 nm).

Fig. S21 Fluorescence decay for compound 2 in the presence of CrO_4^{2-} (λ_{ex} = 300 nm).

Fig. S22 Fluorescence decay for compound 2 in the presence of UO_2^{2+} (λ_{ex} = 300 nm).

Fig.S23 Fluorescence decay for compound 2 in the presence of NFT (λ_{ex} = 300 nm).

Scheme S1. The structures of selected antibiotics.

1. Experimental section

X-ray crystallography

Suitable single crystals of the seven compounds were performed on Bruker APEX D8 QUEST diffractometer with a Photon 100 CMOS detector (Mo-Kα radiation, λ = 0.71073 Å). SADABS and SAINT programs were applied for absorption correction and data processing. The structures were solved by direct methods and refined with full-matrix least-squares on F^2 using the SHELXTL-2014 software package.[1] All the non-hydrogen atoms were refined anisotropically. The hydrogen atoms of organic ligands were placed in geometrically calculated positions and refined using the riding model. Details of the crystallographic data are listed in Table S1. Selected bond lengths and angles for compounds **1-2** are provided in Table S2. CCDC numbers: 2143928, 2143929 for compounds 1-2, respectively.

Calculations

The calculation of the ligand was performed using the Gaussian 09 program. The structure was completely optimized to the ground state by the DFT method at D-B3LYP/6-31G* level. Then the singlet and triplet energy of structures were calculated based on TD-SCF method.

2. Tables

Table S1. Crystallographic Data collection and Refinement result for compounds **1-2**.

Compound reference	**1**	**2**
chemical formula	$C_{50}H_{52}Cd_3N_{16}O_{17}S_2$	$C_{25}H_{34}N_8O_{13}SZn_2$
Crystal system	triclinic	monoclinic
Space group	*P*-1	*C*2/*c*
a /Å	9.0385(15)	18.413(2)
b /Å	10.4711(17)	17.351(2)
c /Å	16.391(3)	20.090(3)
α / º	79.025(5)	90
β / º	82.828(5)	94.808(4)
γ / º	66.964(4)	90
Unit cell volume / Å^3	1399.3(4)	6395.6(13)
Temperature / K	298	298
Z	1	8
μ(mm^{-1})	1.292	1.644
No. of reflections measured	9690	9440
No. of independent reflections	6390	7374
R_{int}	0.0556	0.0237
Final R_1 values ($I > 2\sigma(I)$)	0.0371	0.0279
Final $wR(F^2)$ values ($I > 2\sigma(I)$)	0.0891	0.0732
Final R_1[a] values (all data)	0.0429	0.0303
Final $wR(F^2)$[b] values (all data)	0.0937	0.0751
Goodness of fit on F^2	1.094	1.080

[a] $R_1 = \Sigma||F_o| - |F_c||/\Sigma|F_o|$. [b] $wR_2 = \Sigma[w(F_o^2 - F_c^2)^2]/\Sigma[w(F_o^2)^2]^{1/2}$.

Table S2. Selected bond lengths (Å) and angles (deg) for compounds **1-2**.

Compound **1**							
Cd1 O6	2.377(3)	Cd1 $N1^{ii}$	2.312(3)	Cd1 $N6^{i}$	2.307(3)	Cd2 $O1^{iv}$	2.392(3)
Cd2 O4	2.266(2)	Cd2 $O5^{v}$	2.299(3)	Cd2 $O8^{iv}$	2.429(3)	Cd2 N3	2.301(4)
Cd2 $N8^{v}$	2.302(3)						
$N1^{iii}$ Cd1 $O6^{i}$	91.22(10)	$N6^{i}$ Cd1 $O6^{i}$	86.43(11)	$N8^{v}$ Cd2 $O1^{iv}$	92.79(11)	$O1^{iv}$ Cd2 $O8^{iv}$	54.26(8)
$N1^{ii}$ Cd1 $O6^{i}$	88.78(10)	N6 Cd1 $O6^{i}$	93.57(11)	$N8^{v}$ Cd2 $O8^{iv}$	84.56(10)	O4 Cd2 $O1^{iv}$	95.25(9)
$N1^{ii}$ Cd1 $N1^{iii}$	180.000	N6 Cd1 O6	86.43(11)	$O5^{v}$ Cd2 $O1^{iv}$	149.95(10)	O4 Cd2 $O5^{v}$	113.45(10)
N3 Cd2 $O1^{iv}$	90.92(12)	$N6^{i}$ Cd1 $N1^{ii}$	91.88(10)	$O5^{v}$ Cd2 $O8^{iv}$	95.73(10)	O4 Cd2 $O8^{iv}$	147.15(9)
N3 Cd2 $O8^{iv}$	87.18(12)	$N6^{i}$ Cd1 $N1^{iii}$	88.12(10)	$O5^{v}$ Cd2 N3	88.96(13)	O4 Cd2 N3	107.25(12)
N3 Cd2 $N8^{v}$	166.61(13)	$N6^{i}$ Cd1 N6	180.000	$O5^{v}$ Cd2 $N8^{v}$	81.41(12)	O4 Cd2 $N8^{v}$	85.22(10)
$O6^{i}$ Cd1 O6	180.000						
Compound **2**							
Zn1 O1	1.9210(14)	Zn1 $N1^{i}$	1.9920(14)	Zn2 O1	1.9158(13)	Zn2 $N3^{iii}$	2.0310(17)
Zn1 O10	1.9388(13)	Zn1 N4	2.0167(15)	Zn2 $O12^{ii}$	2.0328(17)	Zn2 $N8^{iv}$	2.0102(15)
O1 Zn1 O10	100.91(6)	O1 Zn1 $N1^{i}$	109.28(6)	O1 Zn2 $N3^{iii}$	108.43(6)	O10 Zn1 $N1^{i}$	124.61(6)
O1 Zn2 $O12^{ii}$	106.65(7)	O1 Zn1 N4	110.92(6)	O1 Zn2 $N8^{iv}$	103.34(6)	O10 Zn1 N4	101.37(6)
$N1^{i}$ Zn1 N4	109.13(6)	$N3^{iii}$ Zn2 $O12^{ii}$	97.15(7)	$N8^{iv}$ Zn2 $O12^{ii}$	134.24(7)	$N8^{iv}$ Zn2 $N3^{iii}$	105.21(7)

Symmetry codes for **1**:(i) -x, 2-y, 2-z; (ii) 1-x, 1-y, 2-z; (iii) -1+x, 1+y, z; (iv) x, 1+y, z; (v) -x, 1-y, 1-z; (vi) x, -1+y, z; (vii) 1+x, -1+y, z. For **2**: (i) 1.5-x, 0.5-y, 1-z; (ii) 0.5-x, 0.5-y, 1-z; (iii) 1-x, -y, 1-z; (iv) -0.5+x, 0.5-y, -0.5+z; (v) 0.5+x, 0.5-y, 0.5+z.

Table S3 Standard deviation and detection limit calculation for UO_2^{2+}, Cr(VI) and NFT in **1**.

	UO_2^{2+}	$Cr_2O_7^{2-}$	CrO_4^{2-}	NFT
1	479673.92	479278.02	479268.75	479865.18
2	479673.85	479278.34	479268.21	479865.75
3	479673.42	479278.92	479269.87	479865.52
4	479673.27	479278.85	479268.93	479865.40
5	479673.32	479278.10	479268.65	479865.14
Standard deviation (σ)	0.306	0.418	0.613	0.251
K_{sv}	4.69×10^3	1.92×10^4	8.03×10^3	1.34×10^4
Detection limit ($3\sigma/K_{sv}$)	1.96×10^{-4}	6.53×10^{-5}	2.29×10^{-4}	5.62×10^{-5}

Table S4 Standard deviation and detection limit calculation for UO_2^{2+}, Cr(VI) and NFT in **2**.

	UO_2^{2+}	$Cr_2O_7^{2-}$	CrO_4^{2-}	NFT
1	536557.86	536539.00	536124.29	537097.14
2	536557.64	536539.42	536124.72	537097.33
3	536557.57	536539.22	536124.63	537097.27
4	536557.25	536539.32	536124.71	537097.24
5	536557.52	536539.72	536124.31	537097.57
Standard deviation (σ)	0.220	0.265	0.215	0.161
K_{sv}	4.86×10^3	1.47×10^4	6.20×10^3	1.02×10^4
Detection limit ($3\sigma/K_{sv}$)	1.36×10^{-4}	5.41×10^{-5}	1.04×10^{-4}	4.74×10^{-5}

Table S5. Comparison of various CPs sensors for the detection of Cr(VI) ions.

	Analyte	CPs-based fluorescent Materials	Quenching constant ($K_{SV}\times 10^4\ M^{-1}$)	Detection Limits (DL)	Ref
1	$Cr_2O_7^{2-}$	$[H_2N(CH_3)_2]_2[Zn_2L(HPO_3)_2]$	39.6	0.116 μM	2
2		$\{[Zn_3(HL)_2H_2O]\cdot 4H_2O\}_n$	50		3
3		$\{[Zn(H_2BCA)(m\text{-}bib)]\cdot H_2O\}_n$	5.3	0.07 μM	4
4		$\{[Zn_2(tpeb)_2(2,3\text{-}ndc)_2]\cdot H_2O\}_n$	7.09	2.623 ppb	5
5		$[Cd(TIPA)_2(ClO_4)_2]$	7.15×10^4	8 ppb	6
		$[Zn(NH_2\text{-}bdc)(4,4'\text{-}bpy)]$	7.62	1.30 μM	7
6		$[Cd_2(L_1)(1,4\text{-}NDC)_2]_n$	5.86	0.031 ppm	8
7		$[Zn_5(TDA)_4(TZ)_4]\cdot 4DMF\}_n$	0.677		9
8		$[Cd_{1.5}(L)_2(bpy)(NO_3)]\cdot 2DMF\cdot 2H_2O$	5.42	320 ppb	10
1	CrO_4^{2-}	$[Cd_{1.5}(L)_2(bpy)(NO_3)]\cdot 2DMF\cdot 2H_2O$	1.73	280 ppb	10
2		$[Zn_2(TPOM)(NDC)_2]\cdot 3.5H_2O$	0.781	2.50 μM	11
3		$\{[Zn(L)_{0.5}(bimb)]\cdot 2H_2O\cdot 0.5(CH_3)_2NH\}_n$	5.04	0.60 μM	12
4		$[Ni(ppvppa)(5\text{-}NO_2\text{-}1,3\text{-}BDC)(H_2O)]\cdot 0.5MeCN$	21.05	0.09 ppb	13
5		$\{[Cd_2L_2(H_2O)_4]\cdot H_2O\}_n$	1.21	3.8 μM	14
6		$\{[Zn_2L_2(H_2O)_4]\cdot H_2O\}_n$	1.95	2.3 μM	

Table S6. Comparison of various CPs sensors for the detection of UO_2^{2+}ion.

	Analyte	CPs-based fluorescent Materials	Quenching constant ($K_{SV}\times 10^4\ M^{-1}$)	Detection Limits (DL)	Ref
1	UO_2^{2+}	$[Eu_2(TATAB)_2]\cdot 4H_2O\cdot 6DMF$	8.4	0.9 μM	15
2		$[Tb(BPDC)_2]\cdot(CH_3)_2NH_2$ (DUT-101)	1.03	8.34 mg/L	16
3		Tb-FAP/agar	24.7	7.95 nM	17
4		$[Zn(HL)(bipy)_{0.5}(H_2O)]\cdot 2H_2O$	4.0	0.4 μM	18
5		$[EuL_{1.5}(H_2O)_2]\cdot 1.75H_2O$	0.371		19
		$[Co_2(dmimpym)(nda)_2]_n$	1.1		20
6		(CH3)2NH2[Eu2(BTC)(AC)3(FM)]	0.856	4.12 μM	21
7		$[Eu_2(MTBC)(OH)_2(DMF)_3(H_2O)_4]$	0.363	309.2 μg/L	22
8		$[Zn(HBTC)(BMIOPE)\cdot DMF\cdot H_2O]_n$	2.29	2.47×10^{-5} M	23
		$\{[Cd_3(TIYM)_2(5\text{-}SASS)_2(H_2O)_2]\cdot H_2O\}_n$	0.469	1.96×10^{-4} M	This work
		$\{[Zn_2(TIYM)(5\text{-}SASS)(\mu_2\text{-}OH)]\cdot 5H_2O\}_n$	0.486	1.36×10^{-4} M	

Table S7. Comparison of various CPs sensors for the detection of NFT.

	Analyte	CPs-based fluorescent Materials	Quenching constant ($K_{SV}\times 10^4\ M^{-1}$)	Detection Limits (DL)	Ref
1	NFT	$[Zn(L)_2]\cdot CH_2Cl_2\cdot CH_3OH$	1.58		18
		$\{[Tb(TATMA)(H_2O)\cdot 2H_2O\}_n$	3.35		19
		$[Cd(tptc)_{0.5}(o\text{-}bimb)]_n$	3.4		20
2		$[Cd(H_2tptc)_{0.5}(mbimb)(Cl)]_n$	26		20
3		$\{[Cd_3(TDCPB)\cdot 2DMAc]\cdot DMAc\cdot 4H_2O\}_n$	10.5		21
		$[Zn_2(azdc)_2(dpta)]\cdot(DMF)_4$	7.14		22

3. Figures

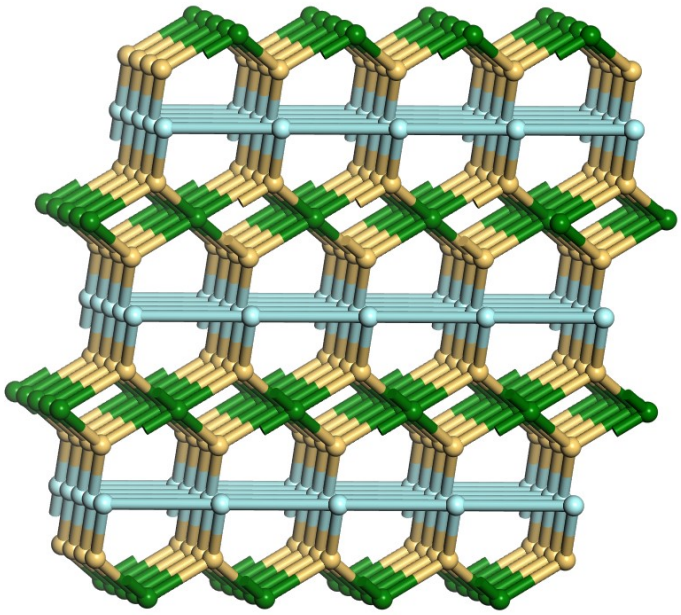

Fig. S1 The simplified network of compound **1**.

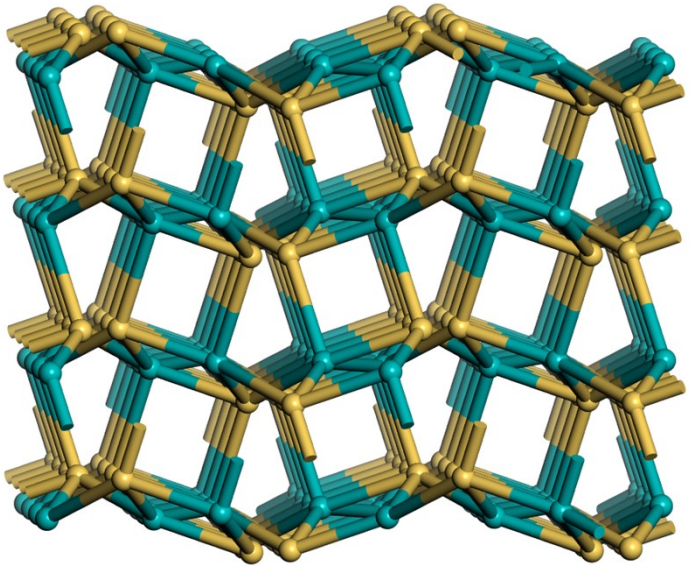

Fig. S2 4,5-connected 3D network of compound **2**.

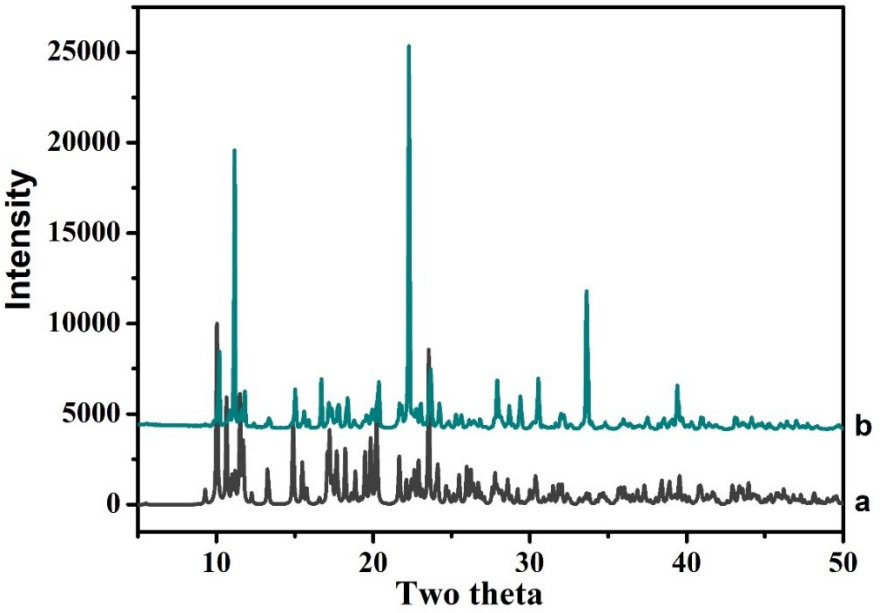

Fig. S3 PXRD pattern of compound **1**: (a) simulated, (b) experimental.

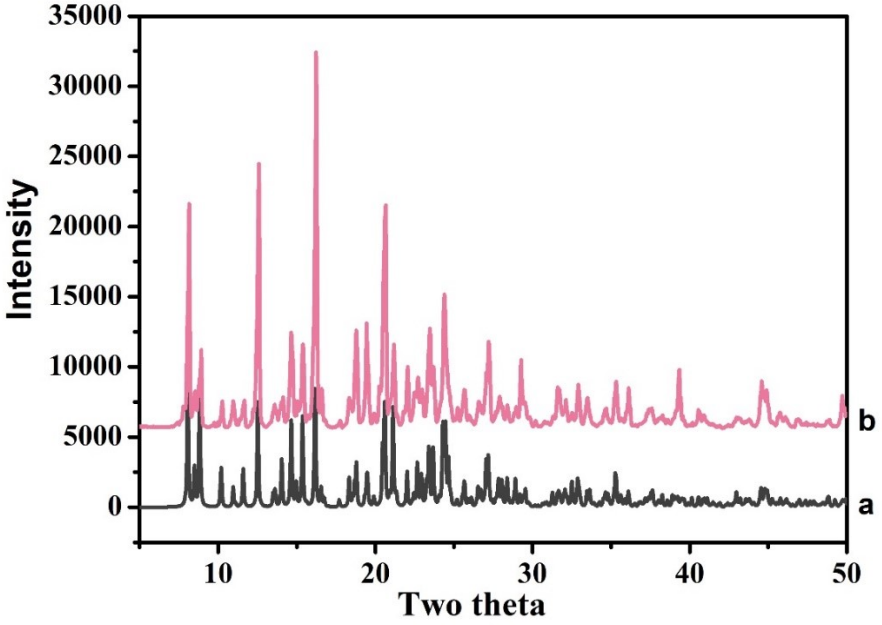

Fig. S4 PXRD pattern of compound **2**: (a) simulated, (b) experimental.

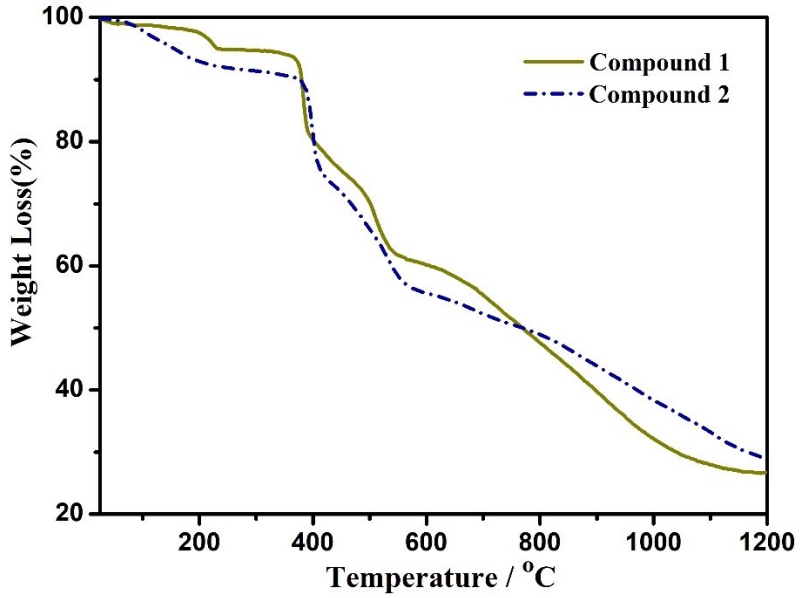

Fig. S5 TGA curves for compounds **1-2**.

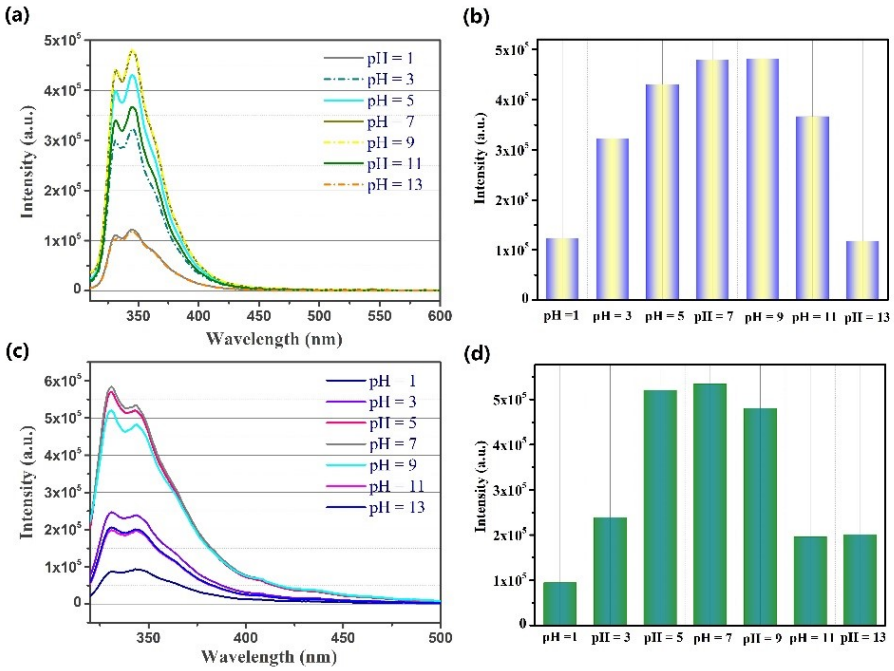

Fig. S6 pH-dependent emission spectra of compound 1 (a) and compound 2 (c) in the aqueous solution with pH ranging from 1 to 13; Histogram showed fluorescence emission of compound 1 (b) and compound 2 (d) at different pH values.

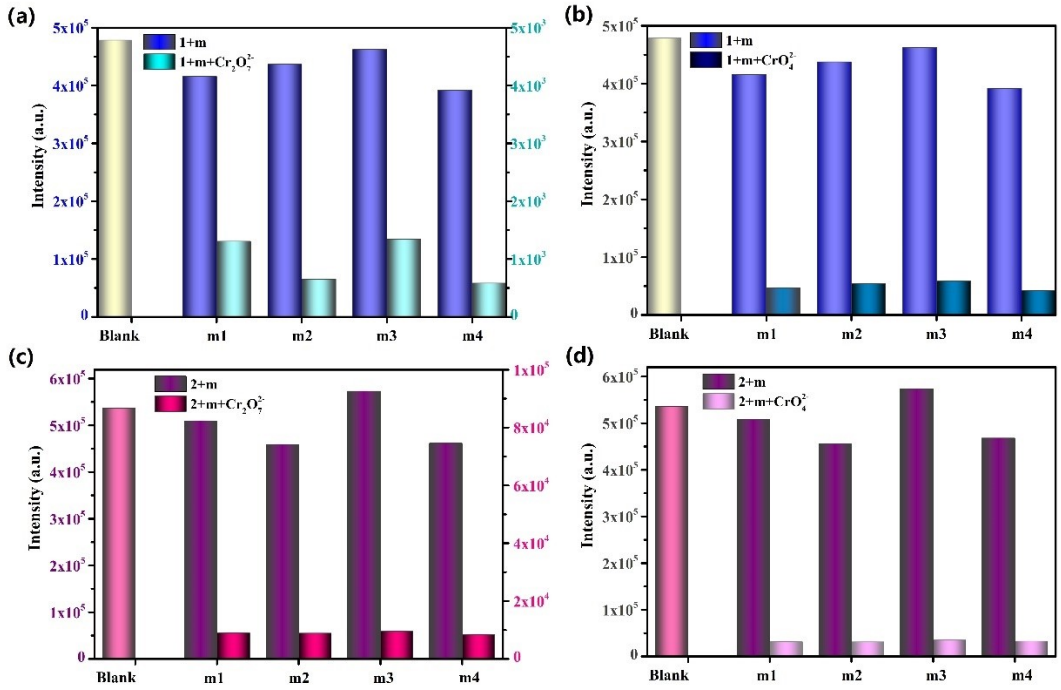

Fig. S7 Luminescence intensities of compound 1 (a, c) and 2 (b, d) with different mixed ions solution added $Cr_2O_7^{2-}$ / CrO_4^{2-} anions (m1: PO_4^{3-} / HPO_4^{2-}; m2: CO_3^{2-} / HCO^{3-}; m3: SO_4^{2-} / $C_2O_4^{2-}$; m4: SCN^- / NO_3^-; 1 mM).

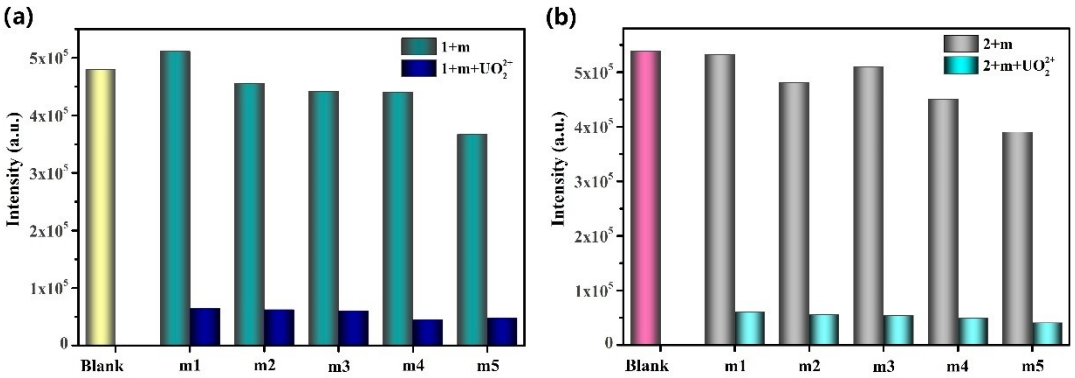

Fig. S8 Luminescence intensities of compound 1 (a) and 2 (b) with different mixed ions solution added UO_2^{2+} ion (m1: K^+ / Ca^{2+} / Mg^{2+}; m2: Zn^{2+} / Cd^{2+}; m3: Co^{2+} / Ni^{2+}; m4: Ag^+ / Na^+; m5: Cr^{3+} / Cu^{2+}; 1 mM).

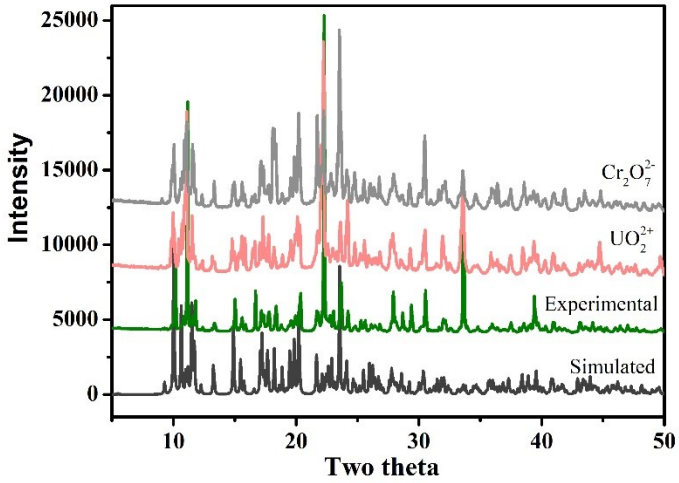

Fig. S9 PXRD pattern of compound 1 after immersing into water with different analytes.

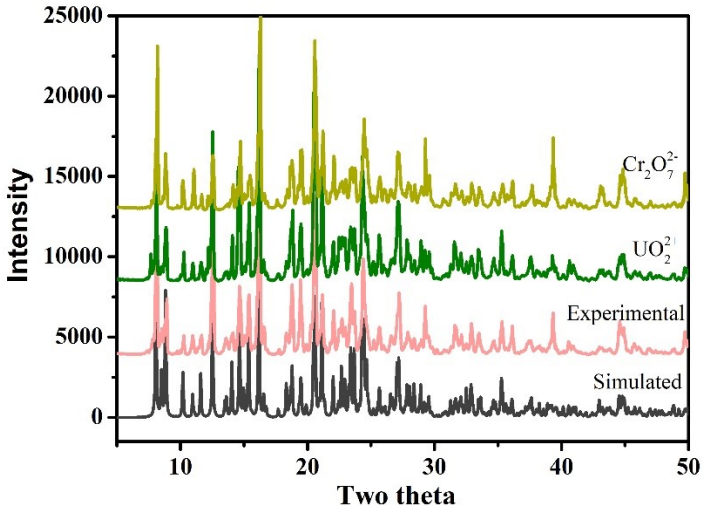

Fig. S10 PXRD pattern of compound 2 after immersing into water with different analytes.

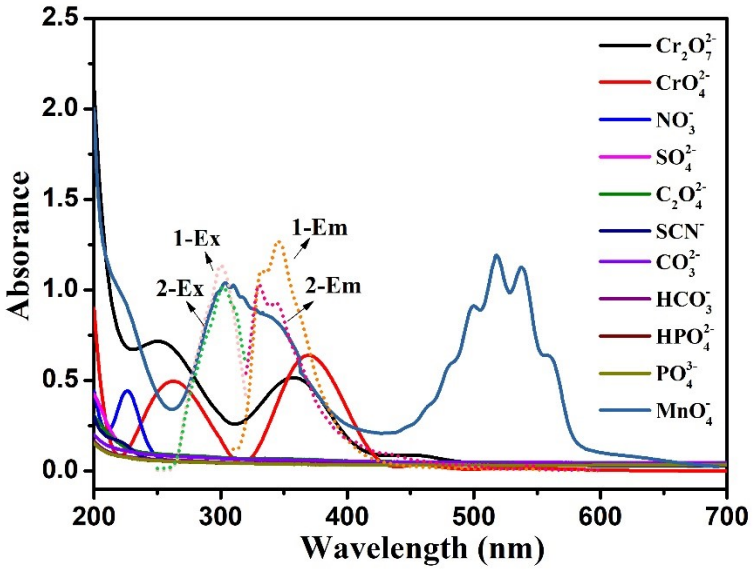

Fig. S11 UV-vis spectra of different anions in aqueous solutions, and the excitation and emission spectra of compounds 1-2.

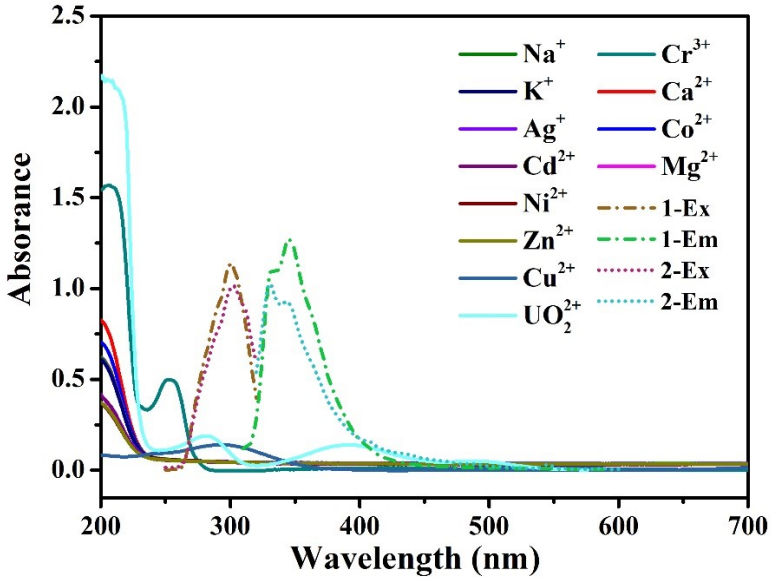

Fig. S12 UV-vis spectra of different metal ions in aqueous solutions, and the excitation and emission spectra of compounds 1-2.

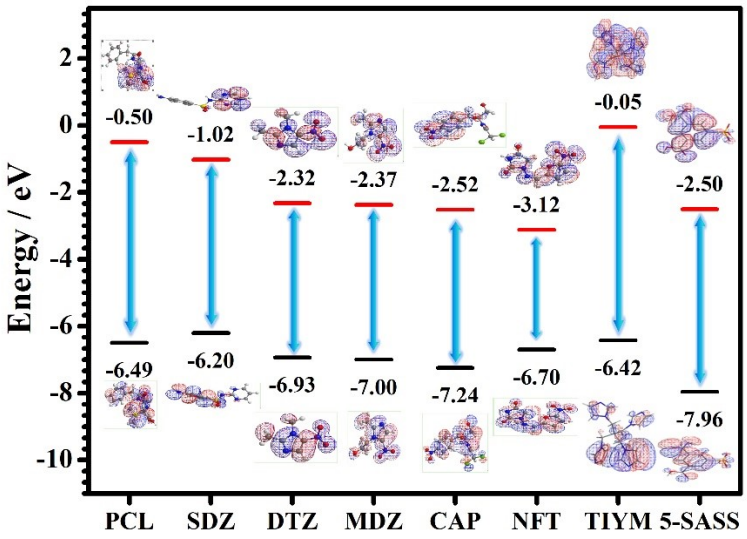

Fig. S13 The HOMO and LUMO energy levels for different antibiotics and ligands.

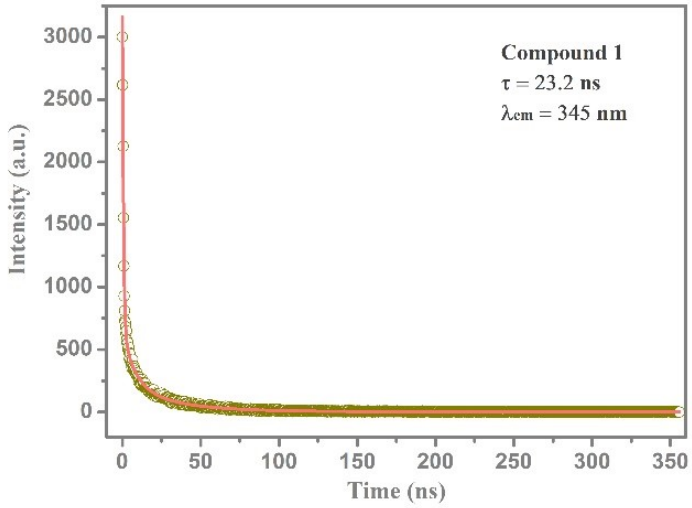

Fig. S14 Fluorescence decay for compound 1 (λ_{ex} = 300 nm).

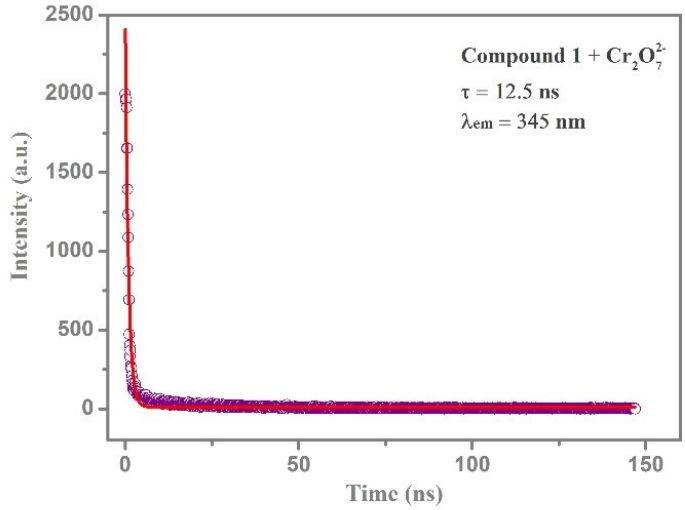

Fig. S15 Fluorescence decay for compound 1 in the presence of $Cr_2O_7^{2-}$.

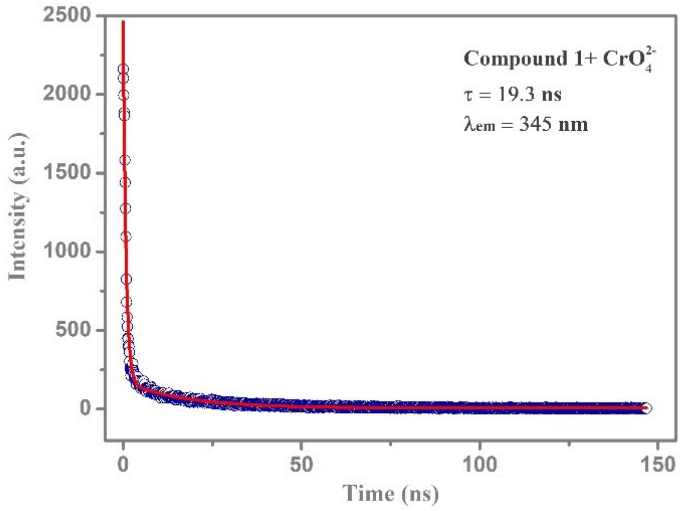

Fig. S16 Fluorescence decay for compound 1 in the presence of CrO_4^{2-} (λ_{ex} = 300 nm).

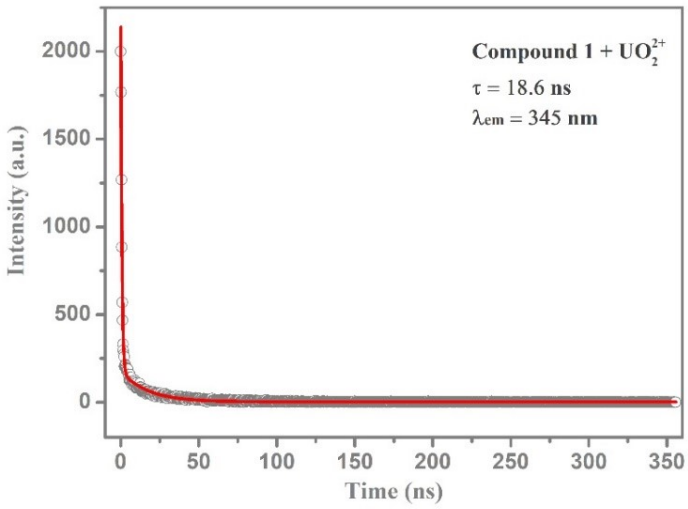

Fig. S17 Fluorescence decay for compound 1 in the presence of UO_2^{2+} (λ_{ex} = 300 nm).

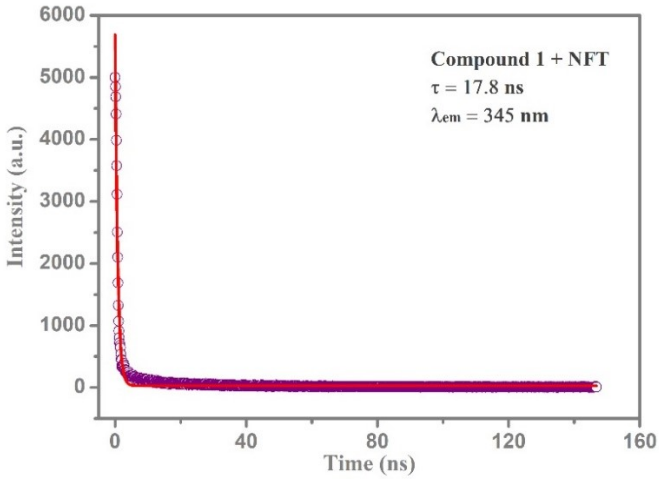

Fig. S18 Fluorescence decay for compound 1 in the presence of NFT (λ_{ex} = 300 nm).

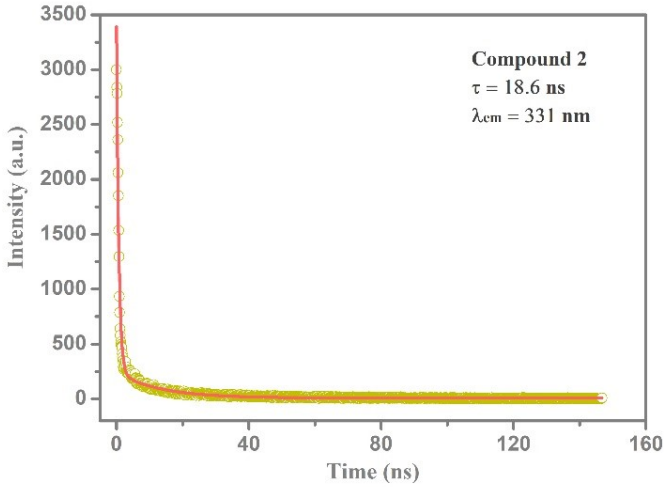

Fig. S19 Fluorescence decay for compound 2 (λ_{ex} = 300 nm).

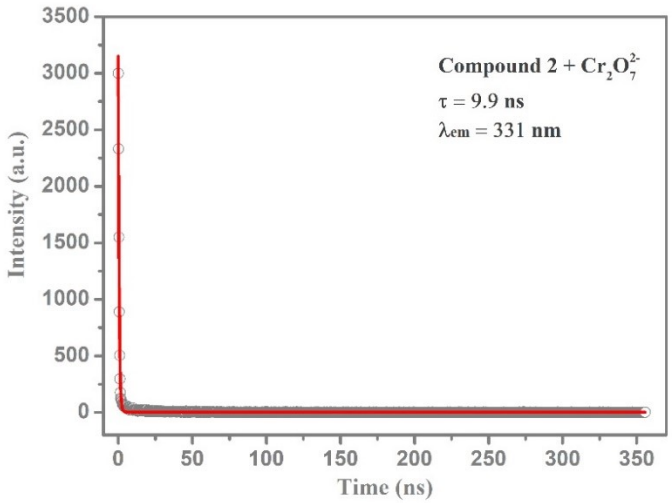

Fig.S20 Fluorescence decay for compound 2 in the presence of $Cr_2O_7^{2-}$ (λ_{ex} = 300 nm).

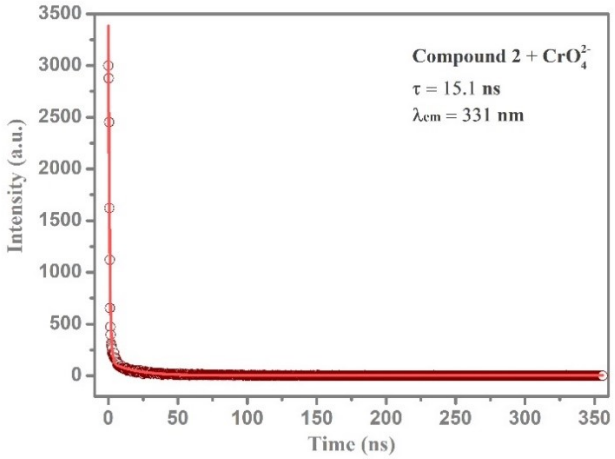

Fig. S21 Fluorescence decay for compound 2 in the presence of CrO_4^{2-} (λ_{ex} = 300 nm).

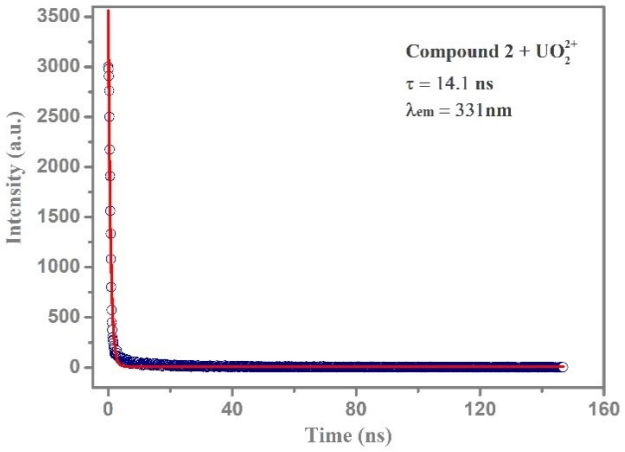

Fig. S22 Fluorescence decay for compound 2 in the presence of UO_2^{2+} (λ_{ex} = 300 nm).

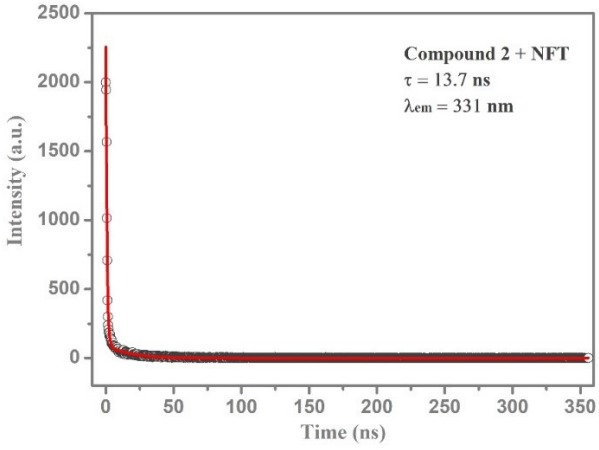

Fig.S23 Fluorescence decay for compound 2 in the presence of NFT (λ_{ex} = 300 nm).

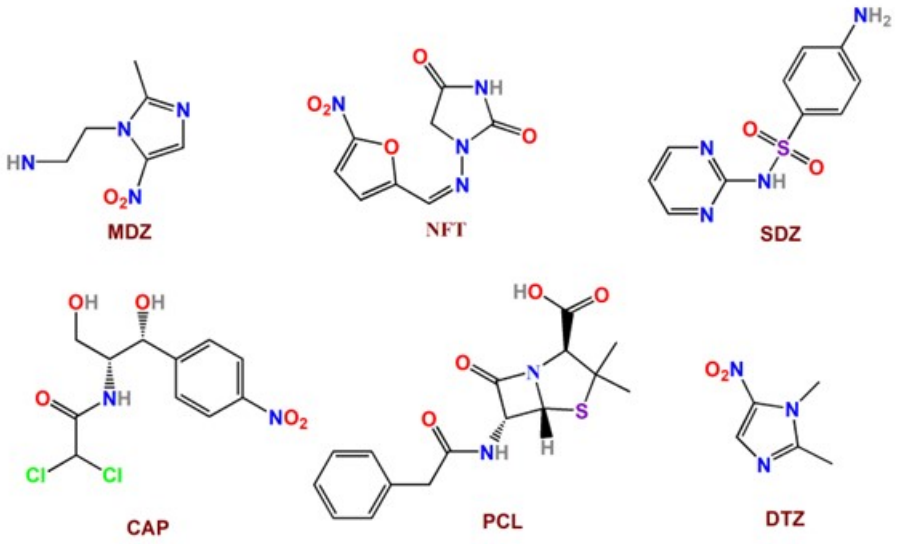

Scheme S1. The structures of selected antibiotics.

Reference:

1. G. M. Sheldrick, *Acta Crystallog C* 2015, **71**, 3.

2. S.-F. Tang and X. Hou, *Cryst. Growth Des*., 2019, **19**, 45.

3. W.-Q. Tong, W.-N. Liu, L.-L. Ma, Y. Wang, J.-M. Wang, L. Hou, Y.-Y. Wang, *Dalton Trans*., 2019, **48**, 7786.

4. X. Zhang, H. Chen, B. Li, G. Liu and X. Liu, *CrystEngComm*., 2019, **21**, 1231.

5. T. Y. Gu, M. Dai, D. J. Young, Z. G. Ren, J. P. Lang, *Inorg. Chem*., 2017, **56**, 4668.

6. H. R. Fu, Y. Zhao, Z. Zhou, X. G. Yang, L. F. Ma, *Dalton Trans*., 2018, **47**, 3725.

7. T. Wiwasuku, J. Boonmak, K. Siriwong, V. Ervithayasuporn and S. Youngme, *Sensor Actuat B-Chem*., 2019, **284**, 403.

8. Y.-J. Yang, Y.-H. Li, D. Liu and G.-H. Cui, CrystEngComm., 2020, 22, 1166.

9. J.-Y. Zou, L. Li, S.-Y. You, H.-M. Cui, Y.-W. Liu, K.-H. Chen, Y.-H. Chen, J.-Z. Cui and S.-W. Zhang, Dyes Pigments., 2018, 159, 429.

10. M. Singh, S. Senthilkumar, S. Rajput and S. Neogi, Inorg. Chem., 55 2020, 59, 3012.

11. R. Lv, H. Li, J. Su, X. Fu, B. Yang, W. Gu and X. Liu, Inorg. Chem., 2017, 56, 12348.

12. C. Xu, C. Bi, Z. Zhu, R. Luo, X. Zhang, D. Zhang, C. Fan, L. Cui and Y. Fan, CrystEngComm., 2019, 21, 2333.

13. X. Zhou, Y.-X. Shi, C. Cao, C.-Y. Ni, Z.-G. Ren, D. J. Young and J.-P. Lang, Cryst. Growth Des., 2019, 19, 3518.

14. C.-X. Wang, Y.-P. Xia, Z.-Q. Yao, J. Xu, Z. Chang and X.-H. Bu, Dalton Trans., 2019, 48, 387.

15. L. Li, S. Shen, J. Su, W. Ai, Y. Bai, H. Liu, *Anal. Bioanal. Chem.*, 2019, **411**, 4213.

16. J. Ye, R. F. Bogale, Y. Shi, Y. Chen, X. Liu, S. Zhang, Y. Yang, J. Zhao, and G. Ning, *Chem. Eur. J*., 2017, **23**, 7657.

17. H. Liu, X. Wang, T. Abeywickrama, F. Jahanbazi, Z. Min, Z. Lee, J.Terry and Y. Mao, *Environ. Sci.: Nano*, 2021, **8**, 3711.

18. J.-X. Hou, J.-P. Gao, J. Liu, X. Jing, L.-J. Li, J.-L. Du, *Dyes. Pigments*., 2019, **160**, 159.

19. Y. Wang, S.-H. Xing, F.-Y. Bai, Y.-H. Xing, and L.-X. Sun, *Inorg. Chem*., 2018, **57**, 12850.

20. W.-M. Chen, X.-L. Meng, G.-L. Zhuang, Z. Wang, M. Kurmoo, Q.-Q. Zhao, X.-P. Wang, B. Shan, C.-H. Tung and D. Sun, *J. Mater. Chem. A*., 2017, **5**,13079.

21. M. Wang, G. Zeng, X. Zhang, F. Y. Bai, Y. H. Xing, Z. Shi, *J. Mol. Struct*., 2021, **1238**, 130422.

22. W. Liu, Y. Wang, L. Song, M. A. Silver, J. Xie, L. Zhang, L. Chen, J. Diwu, Z. Chai, S. Wang, *Talanta*, 2019, **196**, 515.

23. N.-N. Chen, J. Wang, *Appl Organomet Chem*., 2020, **34**, e5743.

24. Y. Liu, Y. Zhao, Z.-Q. Liu, X.-H. Liu, X.-D. Zhang and W.-Y. Sun, *CrystEngComm*., 2020, **22**, 304.

25. Q.-Q. Zhu, H. He, Y. Yan, J. Yuan, D.-Q. Lu, D.-Y. Zhang, F. Sun and G. Zhu, *Inorg. Chem*., 2019, **58**, 7746.

26. Y. Zhang, J. Yang, D. Zhao, Z. Liu, D. Li, L. Fan and T. Hu, *CrystEngComm*., 2019, **21**, 6130.

27. Q.-Q. Zhu, Q.-S. Zhou, H.-W. Zhang, W.-W. Zhang, D.-Q. Lu, M.-T. Guo, Y. Yuan, F. Sun and H. He, *Inorg. Chem*., 2020, **59**, 1323.

28. R. Goswami, S. C. Mandal, N. Seal, B. Pathak and S. Neogi, *J. Mater. Chem. A*., 2019, **7**, 19471.